Analusis, **2000**, *28*, 864-871

Scanning electron microscopy and energy dispersive spectrometric microanalysis of crystalline deposits following evaporation of CO_3H^-, Mg^{2+} and Ca^{2+} containing aqueous solutions

J.-É. Surlève-Bazeille[1*], M. Mercier[1], R. Tarroux[2], A. Mavon[2], E. Neuzil[3], D. Licu[2] and P. Dupuy[2]

[1] *Laboratoire des facteurs de défense et de régulation cellulaire, Université Bordeaux 1, avenue des Facultés, 33405 Talence Cedex, France*
[2] *Institut de recherche Pierre Fabre, allées Camille Soula, Vigoulet-Auzil, BP 82, 31322 Castanet Tolosan Cedex, France*
[3] *Université Victor Segalen Bordeaux 2, 146, rue Léo Saignat, 33000 Bordeaux, France*

Abstract. This paper is the first application of scanning electron microscopy (SEM) and of energy dispersive selection microanalysis (EDS) to the study of natural spa waters used as sprays in current dermatological practice; the aim was to relate the mineral composition of the spray to the sensitory perception recorded by the patients. Crystallized deposits were first obtained on a collodion film, from two spa waters mainly containing hydrogenocarbonate, calcium and magnesium ions, but differing by their Mg/Ca ratio. In order to understand the types of crystals formed, mineral solutions of simpler composition were prepared and submitted to the same process. Among the crystalline varieties of calcium carbonate, calcite and vaterite were characterized; aragonite could not be detected in spa waters deposits, despite the presence of magnesium, which favours the crystallization of this orthorhombic form in the artificial solutions.

Keywords. Scanning electron microscopy (SEM) – energy dispersive selection microanalysis (EDS) – bicarbonated (hydrogenocarbonated) spa waters – Calcium carbonate crystallization.

Introduction

A comparison between four spa spring waters, currently used in dermatological practice as topicals, has been recently performed by determining the sensory profiles obtained from female volunteers after spraying the skin of their cheeks in standard conditions [1]; skin suppleness and comfort were preferably obtained with sprays having a low mineral content, whereas waters with a higher mineral concentration led to a mild pricking[1]. The influence of the different chemical components of these spa waters has not been considered by the authors and one may wonder whether the perceptions recorded are related to the crystallized inorganic deposits that remain on the skin once the water evaporates.

We have therefore tried to visualize and characterize these deposits on different surfaces: collodion membranes, glass, graphite, human skin squamæ and lyophilized human skin. Our preliminary experiments indicated the complexity of the problem: even in strictly controlled conditions, the morphology and the composition of the deposits are determined not only by the origin of the spa water, as suspected, but also by the nature of the surface on which the evaporation was conducted; for instance, the role of epitaxy in the crystallization of calcium carbonate has been recently emphasized [2]. The experiments presented in this paper concern mineral deposits on collodion membranes, a surface giving the most reproducible results and well adapted to microanalysis, as collodion membranes are free from any heavy atoms.

The most favourable sensory effects have been noted by Bacle *et al.* [1] with the less mineralized spray, a spa water containing mainly calcium, magnesium and hydrogenocarbonate ions, beside many more inorganic constituents present in small quantities. This specific composition and the large size variation of the droplets deposited by the spray may explain the complex dynamics of evaporation we observed and the difficulty of interpreting the composite crystallisations we encountered.

For a better apprehension of the crystallization process, in addition to the study limited to two spa waters, we have prepared sprays of simpler aqueous hydrogenocarbonate solutions and investigated the morphology and chemical composition of the crystalline deposits resulting from their

*Correspondence and reprints.
Received September 19, 2000; accepted October 3, 2000.
[1] The four French thermal spring waters examined by Bacle *et al.*, listed according to their increasing mineral content, are from Avène (Hérault), La Roche-Posay (Vienne), Vichy (Allier), Uriage (Isère).

Article available at http://analusis.edpsciences.org or http://dx.doi.org/10.1051/analusis:2000158

evaporation. These solutions contain either calcium or magnesium ions or the same two cations present in different [Ca]/[Mg] ratios, encompassing the values determined in the four above-mentionned natural spa waters. This paper concerns the scanning electron microscopic (SEM) and energy dispersive spectrometric (EDS) microanalytical studies of the crystalline deposits.

Material and methods

Natural spa waters

The natural thermal spring waters were obtained from the pharmaceutical trade in their usual form of aluminium cans coated inside with an epoxy resin, and provided with a sprayer. The cans were pierced with a stabber and their content poured into the same type of flasks used for the laboratory prepared solutions.

The major constituents of the four thermal waters are indicated in table I.

The thermal spa waters from Avène and from La Roche-Posay, which are studied in this paper, are named hereafter TW1 and TW2. They were selected for both their low mineral content and their exclusive use in dermatological hydrotherapy.

Artificial mineral solutions

Four artificial hydrogenocarbonate solutions were prepared (Tab. II). Solutions n° 1 and n° 2 contained respectively calcium and magnesium, in concentration ranges similar to TW1. Both calcium and magnesium were present in solutions n° 3 and n° 4, with [Mg]/[Ca] ratios respectively comparable to TW1 and TW2.

The solutions (0.5 l) were prepared at room temperature with water desionized by reverse osmosis (Millipore MilliQ plus). The required quantity of calcium hydroxide (Sigma, C-555) and of basic magnesium carbonate (Fluka, 63062, purum) were mixed with the desionized water under gentle stirring; gaseous carbon dioxide (Union Carbide) was then bubbled until the mixture became clear. The solubilization was followed by pH measurements.

The artificial hydrogenocarbonate solutions thus prepared were then kept in glass flasks provided with a pumping and spraying system (VP 32/40, ring GCMI 24/140, Valois). A special care was observed to guarantee a perfect cleanness and sterility of the flasks, prior to their filling.

Table I. Chemical constitution of four thermal spring waters (simplified). Ionic concentrations are given in mM.

	Avène	*La Roche-Posay*	*Vichy*	*Uriage*
pH	7.5	7.0	6.8	6.8
Dry residue ($mg.l^{-1}$)	248	444	5.119	11.000
Mg^{2+}	1.06	0.20	0.50	5.14
Ca^{2+}	1.47	3.49	3.75	14.97
Na^{+}	0.20	0.43	80.93	102.69
HCO_3^{-}	4.27	6.49	78.29	6.59
Cl^{-}	0.11	0.70	10.07	98.73
SO_4^{2-}	0.26	0.43	1.87	29.79
Mg^{2+}/Ca^{2+}	**0.72**	**0.05**	**0.13**	**0.34**

Preparation of specimens

Aluminium specimen stubs (3 cm^2) were coated with a 0.5 µm collodion membrane. This membrane was obtained by dropping three drops of a 3 % collodion solution in isoamyl acetate onto the cleaned surface of water in a 16 cm diameter basin (≈ 200 cm^2). The coated stubs were dried for 24 hours at 37 °C. The spray was then applied onto the stubs till an amount of about 30 mg of solution per cm^2 and evaporated at room temperature.

The stubs designed for microanalytic study were covered with an amorphous carbon tablet prior to collodion coating, in order to prevent the formation of parasitic spikes arising from the aluminium holder.

Six groups of specimens were realized: 1 to 4 (Tab. II) corresponding to the four saline solutions, 5 and 6 to the natural spa waters TW1 and TW2.

Electron microscopy

Morphoscopic observations were carried out using scanning electron microscopes JEOL Jem 840 A analytic and Philips SEM 515. Topographic secondary electron images were obtained at accelerating voltages of 10 or 15 kV under secondary vacuum. Prior to observation, the surface of the specimens was sputtered with gold. The conducting film is thin enough to be neglected in the conditions of the experiments.

Microanalysis

Energy dispersive selection microanalysis is a non-destructive technique for qualitative elementary analysis of the area under electron microscopic observation. In the case of this study, the spatial resolution of the method varies between of 0.1 µm and 1 µm approximately, following the local conditions. The equipment used was a Noran Instruments Voyager installation, with an ultra-thin window Si(Li) detector, mounted on a JEOL Jem 840 A analytic scanning electron microscope. This device allows the detection and identification of elements of atomic numbers $Z \geq 6$. The probe accelerating voltage was 10 kV. In order to prevent electric charges, the sample surface was sputtered with a nanometer-thick coat of an alloy Au 95 %, Pd 5 %.

Staining method for differentiating calcite and aragonite

The Feigl method [3] described by Kido [4] is based on the reduction of silver and manganese cations by hydroxyle

Table II. Chemical constitution of four artificial mineral solutions.

Solution n°	*pH*	*Mg^{2+} (mM)*	*Ca^{2+} (mM)*	*Analogy with natural spa waters*	*Mg^{2+}/Ca^{2+}*
1	7.02		1.06	Ca concentration in the range of TW1	
2	7.11	0.88		Mg concentration in the range of TW1	
3	5.68	0.88	1.06	Cationic concentration in the range of TW1	0.83
4	5.74	0.05	1.06	[Mg]/[Ca] in the range of TW2	0.04

anions, resulting in the formation of a black insoluble mixture of manganese dioxide and metallic silver. The black deposits characterize aragonite crystals.

Results

Solution n° 1 (Ca)

The crystals obtained after evaporating solution n° 1 belonged to two different morphological groups. Among rhombohedral 10-20 μm crystals, which were the most abundant (Fig. 1a), some smaller ellipsoidal bodies (2-4 μm) were present, either isolated (Fig. 1b) or associated with the rhombohedra. Energy dispersive selection microanalysis showed that both types of crystals contained C, O and Ca (Fig. 2a).

Solution n° 2 (Mg)

The evaporation of the Mg solution led to a completely different morphological aspect of the deposit: a layer of almost jointing rounded clusters of very small crystals (0.1-1 μm), which were often sintered (Fig. 1c). Microanalysis indicated the presence of C, O and Mg, with traces of Na and S (Fig. 2b).

Solution n° 3 (Mg/Ca ≈ 0.83)

The larger forms obtained were polyhedral crystals (5-20 μm), sometimes lacking sharp-cut edges (Fig. 1d); they were dispersed among rounded clusters of small sintered crystals (0.1-1 μm). The polyhedral crystals were often associated with bunches of micrometric crystalline needles (Fig. 1e). C, O and Ca were characterized in the micrometric crystalline needles and in the polyhedra (which also contained Mg, Fig. 2c).

Solution n° 4 (Mg/Ca ≈ 0.04)

The large rhomboedra (2-20 μm) showed sharp-cut edges; ellipsoidal aggregates of crystals were generally associated to give gypsum flower-like images (Fig. 1f); scarse bunches of micrometric needles were also observed (Fig. 1g). Rhombohedra and ellipsoidal forms only contained C, O and Ca, whereas Mg and traces of Na could be detected in gypsum flower-like structures and in the micrometric needles (Fig. 2d).

Spa water TW1

Five different morphological types of crystalline deposits were observed:

– polyhedral 2-10 μm crystals (Fig. 1h), and in their vicinity;

– small chain-forming crystals (0.2–0.3 μm, Fig. 1h), unstable under the electron beam;

– globular crystalline assemblages of 1–3 μm diameter (Fig. 1i);

– a crust of small (0.1 μm) crystals (Fig. 1j) showing a similar aspect as the one given in Fig. 1c;

– gypsum flower-like aggregates (1–2 μm) formed by numerous associated crystalline flakes; the thickness of an elementary flake was less than 0.1 μm (Fig. 1k).

The polyhedral forms and the globular assemblages only contained C, O and Ca; in the chained unstable crystals, only Na and Cl could be characterized; in the crust, C, O, Na, Mg, S, Cl and Si were accompanied by a small quantity of calcium (Fig. 2e).

Spa water TW2

The images obtained are simpler than those observed with TW1, as they showed only three types of crystalline deposits (Fig. 1l):

– large polyhedral, mostly rhombohedral crystals (10-20 μm): they were often connected and contained C, O and Ca;

– small (1 μm) polyhedral crystals; their main constituents were Cl and Na;

– a continuous layer constituting the border left by the evaporated droplets with the presence of C, O, Ca, Mg, Si, Cl and Cu (Fig. 2f).

Comments

Hydrogenocarbonate anions are present in the artificial solutions prepared by bubbling CO_2 as well as in the commercial cans containing the natural thermal waters. It is evident that an important part of carbon dioxide will escape in gaseous form during the spraying process and furthermore during the evaporation step. Nevertheless HCO_3^- remains a

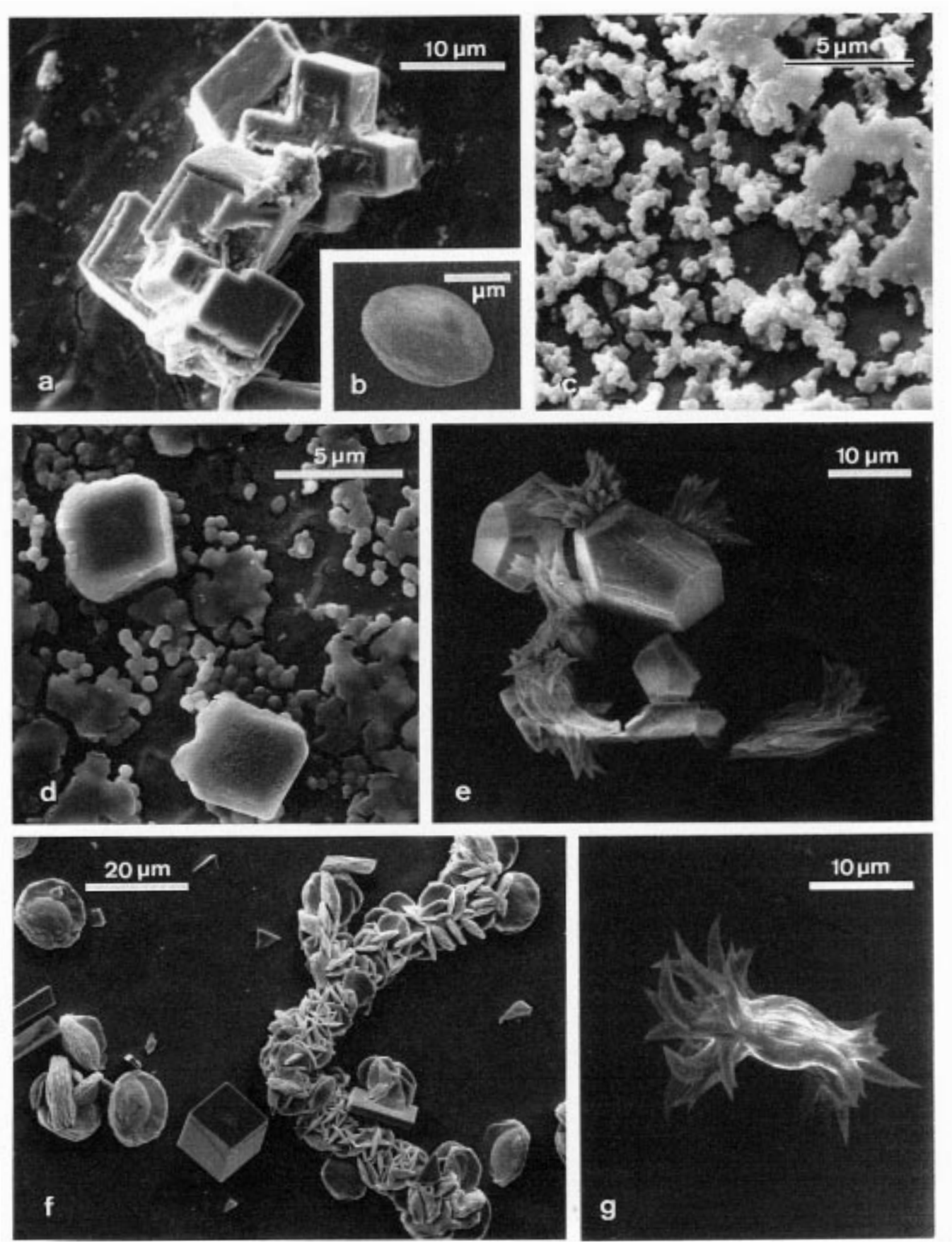
10 µm
µm
a
b
5 µm
c
5 µm
d
10 µm
e
20 µm
f
10 µm
g

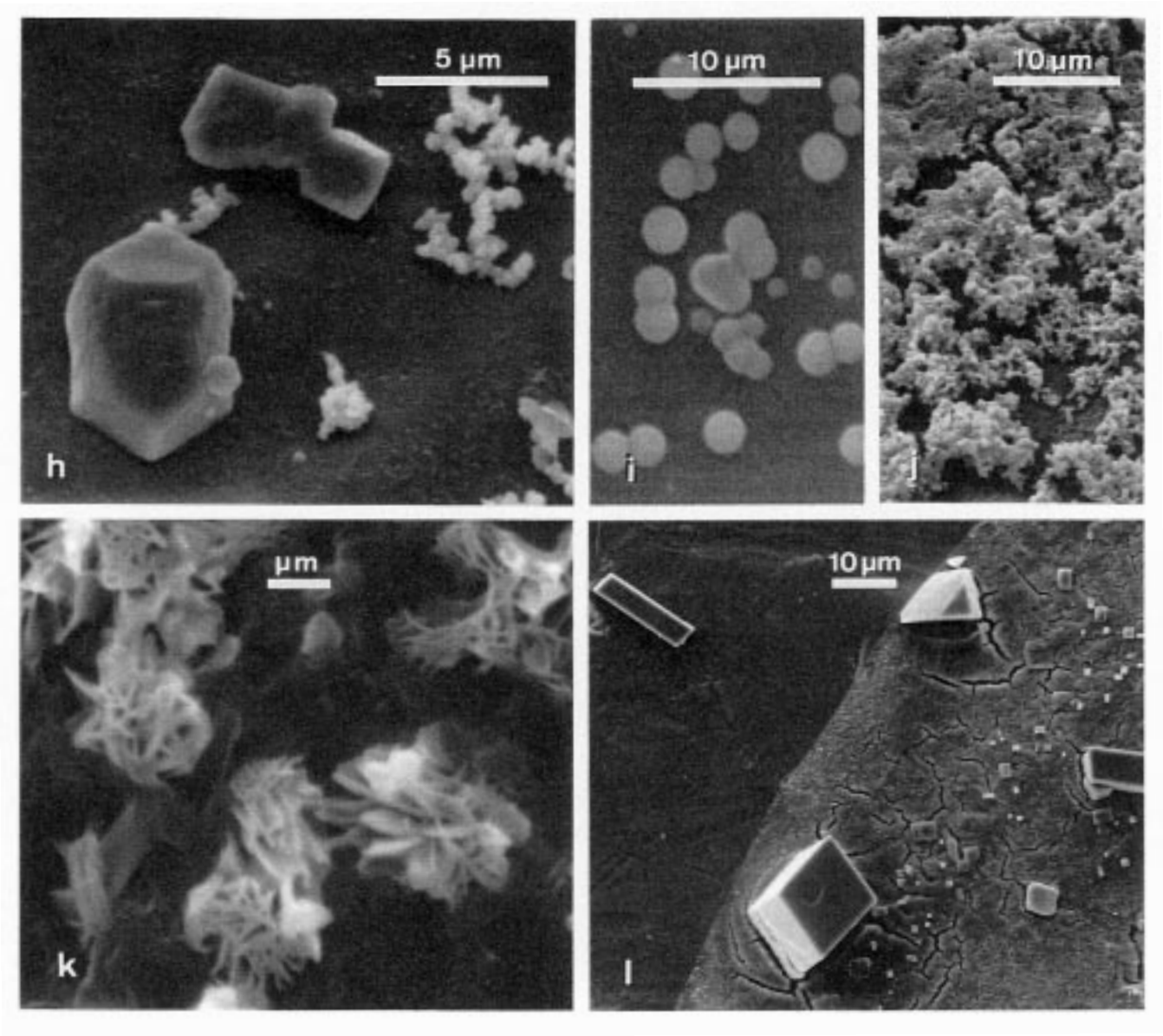

Figure 1. Scanning electron microscopy of the crystalline deposits.
a: calcite rhombohedra; b: ellipsoidal vaterite; c: magnesite; d: distorted calcite polyhedra and smaller crystals of magnesite; e: calcite polyhedra associated with aragonite needles; f: large calcite rhombohedra and gypsum flower-like vaterite; g: bunch of aragonite needles; h, i, j, k: deposits from spa water TW1; l: deposits from spa water TW2.

major ionic constituent, together with Ca^{2+} and Mg^{2+}. The deposits given by the evaporation of natural spa waters (or artificial solutions) must be obviously composed of representatives of the group of neutral calcium or magnesium carbonates; calcium or magnesium hydrogenocarbonates must be excluded, as they have never been isolated [5,6], on account of their instability in the presence of water; only sodium and potassium hydrogenocarbonates may be obtained in crystalline stable form.

Calcium carbonate ($CaCO_3$) is poorly soluble in pure water (14.3 mg/l), despite the fact that a monohydrate and a hexahydrate of calcium carbonate may be obtained in particular conditions [7]. Anhydrous calcium carbonate is polymorphous, existing in an amorphous state and under three major crystallographic forms. The most common and stable form is represented by calcite which belongs to the trigonal (or rhomboedral) system. Aragonite is less common and somewhat less stable than calcite at ordinary pressure and temperature; the unit cell of its crystals falls in the orthorhombic space group. Vaterite (μ-$CaCO_3$) is a third crystalline unstable variety of calcium carbonate, belonging to the hexagonal system; spheroliths and small needles are

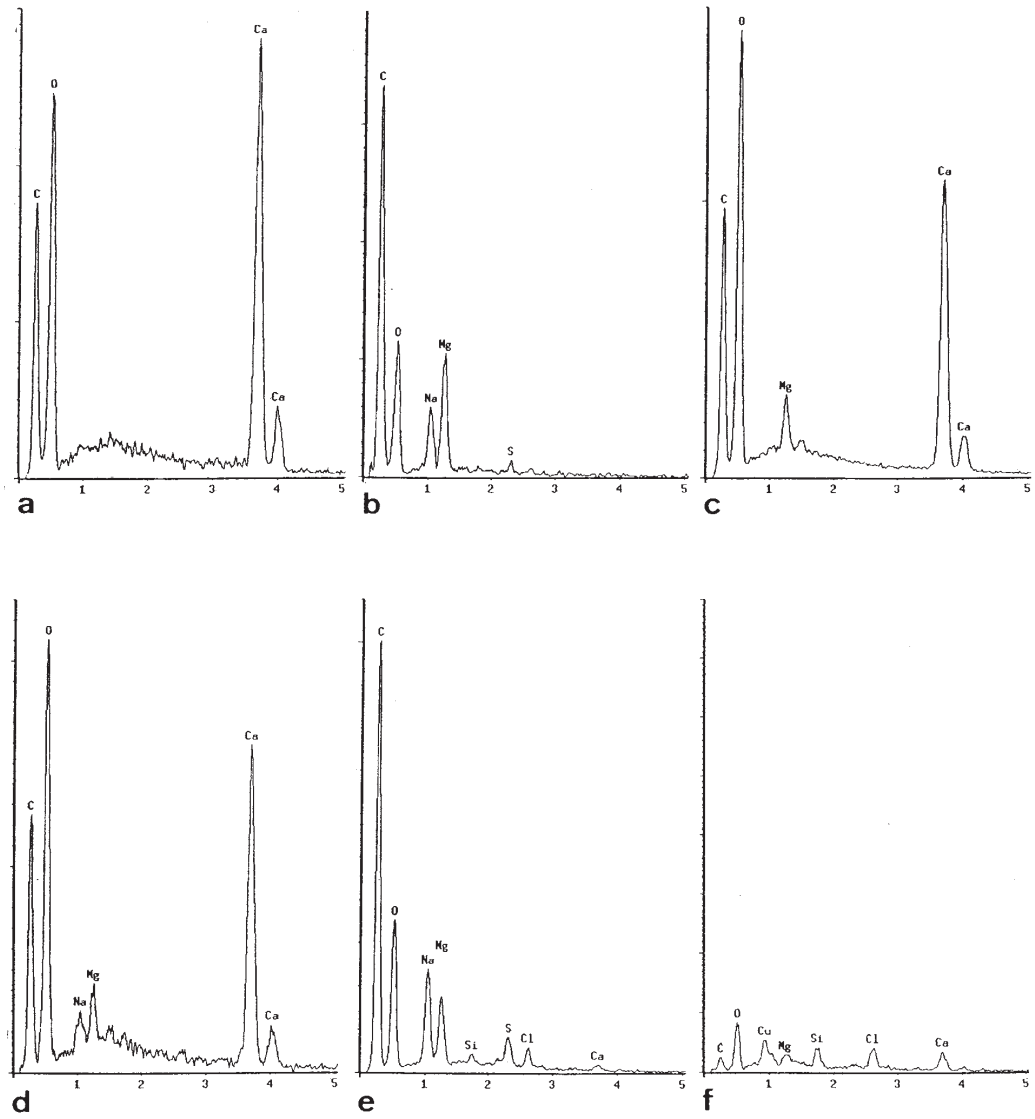

Figure 2. EDS microanalysis of crystalline deposits from solutions n° 1, 2, 3, 4 (spectra a, b, c, d) and from spa waters TW1 and TW2 (spectra e and f). Energy (keV) on X-axes, counts on Y-axes.

the usual morphological aspects of vaterite crystals [8,9]. Magnesite ($MgCO_3$) is the natural form of magnesium carbonate: this metamorphic mineral is rarely pure, as it is usually associated with other metals, specially with iron; powder diffraction patterns let assume that magnesite only differs from calcite by its cell parameters [10]. Dolomite is the mixed neutral carbonate $CaMg(CO_3)_2$; the crystal structure of dolomite resembles that of calcite, with a space group of lower symmetry.

Crystalline deposits from artificial solutions

Calcium carbonate is the only constituent of both types of deposits obtained from solution n° 1. The rhombohedra are the typical crystallization form of calcite. Ellipsoidal deposits are very similar to the images of vaterite obtained in SEM by Cailleau *et al.* [11] and by Rola [12].

The homogeneous deposit characterizing solution n° 2 is formed of magnesium carbonate, very likely precipitated as magnesite. As magnesium carbonate is less insoluble than magnesium hydroxide, the deposit obtained, besides magnesite, probably contains some basic magnesium carbonate, a mixture of $MgCO_3$ and $Mg(OH)_2$. The traces of Na and S originate from the magnesium basic carbonate used to prepare the HCO_3^- containing solution; despite the fact that this compound was commercially sold as a product of high purity, its sodium content was only warranted to be < 0.2 %.

In the deposits of solution n° 3, calcite is easy to characterize on account of its typical large polyhedral crystals; the lack of sharp-cut edges of the rhombohedra may be a consequence of local distortions of the crystal lattice by the incorporation of some magnesium ions. The bunches of needles show the same appearance as the vaterite crystals undergoing a secondary transformation into aragonite, as described by Cailleau *et al.* [11]. It may be assumed that the magnesium carbonate deposit which contains some calcium ions is formed of impure magnesite, possibly partly mixed with dolomite.

In solution n °4 deposits, the rhombohedra are particularly well crystallized and their composition strickly limited to C, O and Ca. This last point suggests that these crystals are made of pure calcite devoided of contamination as the magnesium concentration of the mother solution is low. The bunches of needles (vaterite changing to aragonite) are similar to those described for solution n° 3. The gypsum flower-like aggregates can be identified as vaterite, since our images are very close to those obtained by Rola [12].

Crystalline deposits from natural spa waters

Regarding spa water TW1, the rhombohedra (calcite, as in artificial solutions 1, 3 and 4) and globular forms (vaterite, as in solutions 1 and 3) are two types of deposits with a simple ternary composition, limited to C, O and Ca. The small chain-forming unstable crystals are even more simple: sodium chloride crystals, the corresponding ions of which being effectively present in this native natural thermal water. Finally, two other deposits show a much more complex composition, as C, O and Ca (or Mg) are associated with Si, Na, Cl and S. The magnesium carbonate in the form of layers of small crystals (magnesite) and the calcium carbonate appearing as gypsum flower-like aggregates (vaterite) are both impure, reflecting the complex mineral composition of TW1 spa water [13].

Spa water TW2 deposits show a simpler aspect which allows an easy identification of the largest crystals (calcite, the particularly stable form of calcium carbonate), of the small crystals (sodium chloride) and of the layers of impure magnesite.

Our results with the artificial mineral solutions n° 3 and n° 4 confirm the beneficial influence of magnesium ions on the formation of aragonite noted by Cailleau *et al.* [11], who also showed that some magnesium ions can be incorporated into calcite crystals; the frited edges of the calcite crystals observed in those solutions may be considered as the induced distortion of the original crystal lattice of the pure calcite crystals. As Cailleau *et al.* [11], we have also noticed in the same solutions some images of transformation of vaterite into aragonite, a probable consequence of a dissolution-recrystallization process. However, no aragonite could be visualized, either by SEM or by the Feigl technique, in both spa waters TW1 and TW2 deposits, despite the high Mg^{2+} concentration and the high Mg/Ca ratio in TW1 spa water. The favourable effect of magnesium on aragonite formation is probably inhibited by the presence in these natural waters of other ions that influence the separation of calcium carbonate from hydrogenocarbonate solutions [14].

Conclusion

Scanning electron microscopy is now currently used as a tool to study the different crystal forms of calcium carbonate [15-18], associated with EDS analysis [19,20]. To our best knowledge, these techniques have not yet been used in the field of thermal spa waters, especially regarding the crystal agglomerates resulting from evaporating a spray. Our work, in which SEM is associated with energy dispersive selection microanalysis, show the complexity of the deposits.

This paper is a preliminary work realized on collodion film and is a basis for future experimental work on biological material; the role of epitaxy could thus be evaluated. The final aim is however a better understanding of the interaction of the skin with the spa water sprays utilized in dermatological practice, as the influence in skin physiology of Mg^{2+} and of Ca^{2+} [21] and of the ratio Mg/Ca has been recently emphasized [22].

Acknowledgments

We are grateful to Dr. Elisabeth Sellier for her skillful assistance in the microanalytic work.

References

1. Bacle, I.; Meges, S.; Lauze, C.; McLeod, P.; Dupuy, P. *Int. J. Dermatol.* **1999**, *38*, 101-103.
2. Litvin, A. L.; Valiyaveettil, S.; Kaplan, D. L.; Mann, S. *Adv. Mater.* **1997**, *9*(2), 124-127.
3. Feigl, F. *Quantitative analysis by spot test*; Nordemann: New York, 1937, pp 328-329.
4. Kido, T. *Acta Histochem.Cytochem*. **1996**, *29*(2), 121-127.
5. Bénard, J. In *Nouveau Traité de Chimie minérale*; Pascal, P., Ed.; Masson: Paris, 1958; t. IV, pp 520-523.
6. Dupuis, T. In *Nouveau Traité de Chimie minérale*; Pascal, P., Ed.; Masson: Paris, 1958; t. IV, pp 232-233.
7. Brooks, R.; Clark, L. M.; Thurston, E. F. *Phil. Trans. Roy. Soc. London* **1950**, *253A*, 145-147.
8. Dupont, L.; Portemer, F.; Figlarz, M. *J. Mater. Chem.* **1997**, *7*(5), 797-800.
9. Gabrielli, C.; Maurin, G.; Poindessous, G.; Rosset, R. *J. Cryst. Growth* **1999**, *200*(1-2), 236-250.
10. Deer, W. A.; Howie, R. A.; Zussman, M. A. *Rock forming minerals*; Longmans: London, 1963, Vol. 5, pp 226-322.
11. Cailleau, P.; Dragone, D.; Girou, A.; Humbert, L.; Jacquin, C.; Roques, H. *Bull. Soc. fr. Mineral. Cristallog.* **1977**, *100*, 81-88.
12. Rola, M. Sc. D. Thesis, Institut national des Sciences appliquées de Toulouse (France), n° 266, 1994.
13. Neuzil, E.; Cousse, H.; Teissier, J.-L.; Fabre, P. *Bull. Soc. Pharm. Bordeaux* **1995**, *134*, 135-162.
14. Kitano, Y. *Bull. chem. Soc. Japan* **1962**, *35*, 1973-1980.

15. Tazaki, K.; Ishida, H.; Fyfe, W. S. *Clays Controlling Environ., Proc. Int. Clay Conf.*; Churchman, G. J.; Fitzpatrick R. W.; Eggleton, R. A., Eds 10th. meeting of Int. Clay Conf., 07 30 1993; Commonwealth scientific and industrial research organization: Melbourne, 1995; 62LZAG.

16. Collier, A. P.; Hetherington, C.J.D.; Hounslow, M. J. *Chem. Eng. Res. Des.* **1996**, *74*, 759-764.

17. Nassrallah-Aboukais, N.; Boughriet, A.; Fisher, J. C.; Wartel, M.; Langelin, H. R.; Aboukais, A. *J. Chem. Soc., Faraday Trans.* **1996**, *92*(17), 3211-3216.

18. Renaut, R. W.; Jones, B. *Can. J. Earth Sci.* **1997**, *34*(6), 801-818.

19. Díaz-Espiñeira, M.; Escolar, E.; Bellanato, J.; Medina, J. A. *Scanning Microsc.* **1995**, *9*(4), 1071-1079.

20. Zhou, D.; Krauss, A. R.; Gruen, D. M. *J. Appl. Phys.* **1997**, *82*(8), 4051-4054.

21. Guy, R. H.; Hostynek, J. J.; Hinz, R. S.; Lorence, C. R; *Metal and the skin; topical effect and systemic absorption*; Dekker: New York, 1999, pp 103-108 and 257-261.

22. Denda, M.; Katagiri, C.; Hirao, T.; Maruyama, N.; Takahashi, M. *Arch. Dermatol. Res.* **1999,** *291*, 560-563.